# ANALYSIS OF PRETENSION AND STRESS STIFFENING IN A SELF-DEPLOYABLE DEORBITING SPACE STRUCTURE

**Peter R. Lauridsen[(1)], Jan A. Nikolajsen[(2)], Anders S. Kristensen[(3)]**

[(1,2,3)] *Department of Civil Engineering, Aalborg University Esbjerg, Niels Bohrs Vej 8, 6700 Esbjerg, Denmark, Email: prl@civil.aau.dk, jan@civil.aau.dk, ask@civil.aau.dk*

## ABSTRACT

In the development of the Self-deployable Deorbiting Space Structure (SDSS) [1][2] FEA are used to determine the stress state during the folding process of a given rectangular Highly Flexible Frame (HFF). The rectangular HFF is the load carrying structure in the SDSS. The stress state changes during the folding process of the HFF and this paper will determine the critical stress states. One of the important subjects in the stowed SDSS is the amount of stored strain energy in the HFF, and the amount of strain energy causes the pretension of the SDSS. To determine the pretension and stress stiffening in a given HFF, non-linear geometrical FEA are conducted.

## NOMENCLATURE

| | |
|---|---|
| $E$ | = Young's modulus, $MPa$ |
| $V$ | = Volume, $mm^3$ |
| $r$ | = Radius, $mm$ |
| $t$ | = Thickness, $mm$ |
| $h$ | = Height, $mm$ |
| $\varepsilon$ | = Strain |
| $\tau$ | = Shear stress, $MPa$ |
| $\sigma$ | = Normal stress, $MPa$ |
| $\sigma_{11}$ | = Maximum principal stress, $MPa$ |
| $F_R$ | = Force reaction, $N$ |
| $M_R$ | = Moment reaction, $Nmm$ |
| $\theta$ | = Rotation, $rad$ |
| $\alpha$ | = Angle, $rad$ |
| $U$ | = Strain Energy, $J$ |

## 1 INTRODUCTION

Deorbiting satellites after end of operation is important to minimize the risk of collision with space debris or other satellites. UN has proposed some guidelines [3] for Space Debris Mitigation (SDM) as a result of this increasing risk, and this problem is growing due to the increasing number of satellites in orbit. In Low Earth Orbit (LEO) is it possible to use the low air density to achieve drag enough to deorbit satellites [4]. The SDSS use this potential for drag in LEO, and the simplicity and robustness for debris mitigation make it attractive in future satellites. The SDSS can be in hibernation for e.g. 25 years, and the pretension in the HFF is retained to ensure deployment of the drag sail. Deploying large structures like Gossamer sails [5] are similar to the SDSS. The objective is to determine critical stress states and pretension in the HFF during the folding process. FEA of a given HFF will be used to determine stress states and the pretension stored in the structure.

## 2 FOLDING PROCESS OF A GIVEN HFF

FEA are based on a HFF with a radius of 2000 $mm$ and the rectangular dimensions of the cross section are 4 $mm$ in thickness and 10 $mm$ in height. Twisting a circular ring is a well-known principle and the SDSS use these principles to fold the HFF [6]. Fig. 1 shows the principle in folding the HFF where the left side in the circular ring is constrained against rotation in 3 Degrees Of Freedom (DOF). The right side in the circular ring is constrained against rotation in 2 DOF and the last DOF is applied $2\pi$ rotation to obtain the folding.

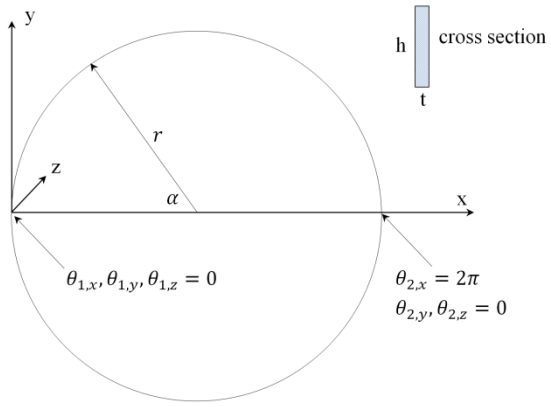


*Figure 1. Principles in folding a HFF. The HFF is fixed in the left side and exposed to a $2\pi$ rotation in the right side.*

During the folding process is the HFF exposed to large deformations and these deformations depend on dimensions of the cross section. In Fig. 2 are the large deformations shown during the folding process. It should be noted that the radius is reduced three times during the folding process. The total strain energy is increasing during the folding, and $M_{R,x} = 0\ Nmm$ when the HFF is folded.

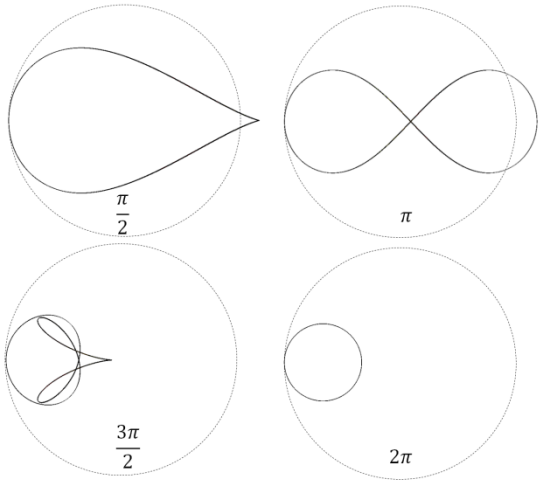


*Figure 2. Deformation of the HFF during the folding process and the undeformed shape is also shown.*

In the folding process are all $F_R = 0\ N$ due to symmetry in the frame. When the HFF is folded the area of the circle is decreased 9 times compared to the original size.

## 3 FEA OF FOLDING A GIVEN HFF

An isotropic material is used to model the HFF, and the cross section is rectangular to obtain the correct folding process. The radius results in an area on $12.6 \cdot 10^6\ mm^2$ for the unfolded SDSS. $E = 2 \cdot 10^5\ MPa$ which is similar to the stiffness of austenitic stainless steel and this material is capable to withstand the hostile environment in space. Dimensions of the cross section are $t = 4\ mm$ and $h = 10\ mm$ and the thickness is orientated in the radial direction. It is assumed that the HFF is without prestress before it is folded. During the folding process, the HFF is exposed to two buckling loads which make the FEA challenging to converge. To achieve good results a structural non-linear geometric FEA is conducted. In order to make convergence easier are contact elements not taken into consideration in the FEA. The HFF is allowed penetrating itself in the FEA however it is in conflict to the physical behaviour. In the FEA are 630 finite shell elements used to model the HFF. The $M_{R,x}$ is increasing rapidly in the first part of the folding process where the rotation is between 0 and $\frac{\pi}{2}$. When the first buckling load is obtained at $\theta_{2,x} \approx \frac{\pi}{2}$ the $M_{R,x}$ is decreasing significant. The varying $M_{R,x}$ during the folding process is shown in Figure 3. [7]

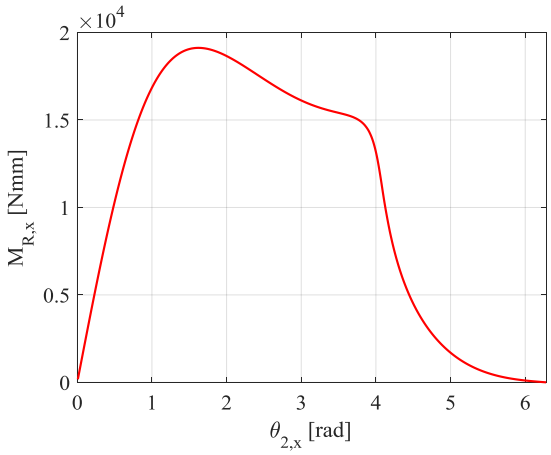


*Figure 3. Rotation of the HFF results in varying $M_{R,x}$.*

Through the folding process the amount of strain energy increases and Eq. 1 shows how to determine it. In the first part of the rotation up till $\frac{4\pi}{3}$ the strain energy is nearly increasing linearly and this is evident in Fig. 4. In Fig. 4 it is illustrated that that the strain energy is almost constant between $\frac{4\pi}{3}$ and $2\pi$ and this is due to the low $M_{R,x}$ in this part of the folding process. The total strain energy is $67\ J$ when the HFF is folded. Analyses and determination of the strain energy is important due to the pretension and stress stiffening in the HFF.

$$U(\theta_x) = \int_0^{\theta_x} M_R(\theta_x)\, d\theta_x = \frac{1}{2}\, V\, E\, \varepsilon(\theta_x)^2 \qquad (1)$$

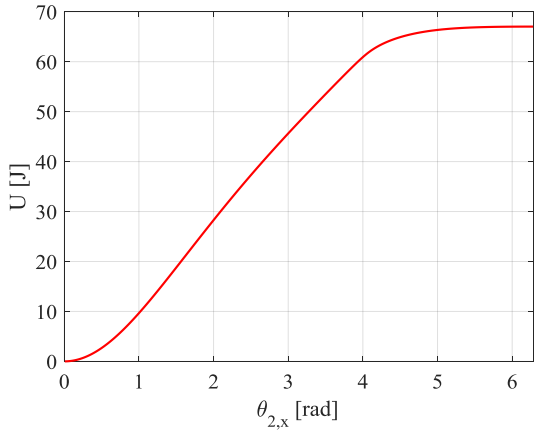


*Figure 4. The folding process of the HFF results in increasing strain energy.*

## 4 STRESS ANALYSIS OF HFF DURING FOLDING PROCESS

Stresses are analyzed during the folding process, and critical points on the HFF are of interest. In the folding process is the HFF exposed to a complex stress state and high stresses are not necessarily equivalent to high $M_{R,x}$. Normal and shear stresses are varying non-linear in the HFF during the folding. Equivalent stresses in the HFF are analysed and certain regions are of interest due to the high stress level. Stresses are retrieved from the nodes. From the FEA it can be concluded that two regions are exposed to a high equivalent stress level during the folding. These regions are denoted point A and point B on the HFF and these are illustrated in Fig. 5. The regions are located in following angles, A: $\alpha = \left[\frac{3\pi}{4}, \frac{5\pi}{4}\right]$ and B: $\alpha = \pi$.

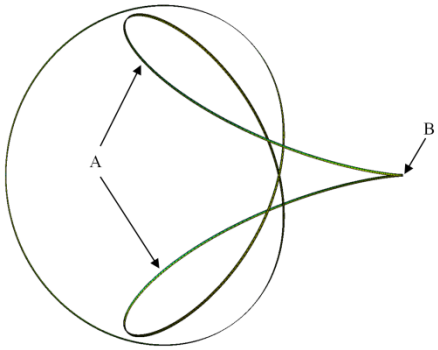


*Figure 5. In this part of the folding process is the equivalent stress level highest in region A.*

In Fig. 6 is it evident that the equivalent stresses are increasing rapidly at the start of the folding process. In point A the equivalent stresses are peaking with 467 $MPa$ when $\theta_{2,x} \approx 4.5\, rad$. However the equivalent stresses are higher in point B during the folding process and it peaks with 489 $MPa$ when $\theta_{2,x} \approx 3\, rad$. After the HFF is folded the equivalent stress are almost uniform in all nodes due to the circular shape and because contact elements are not taken into consideration. The equivalent stress peak in point B, is 22 % higher compared to the equivalent stresses level when the HFF is folded.

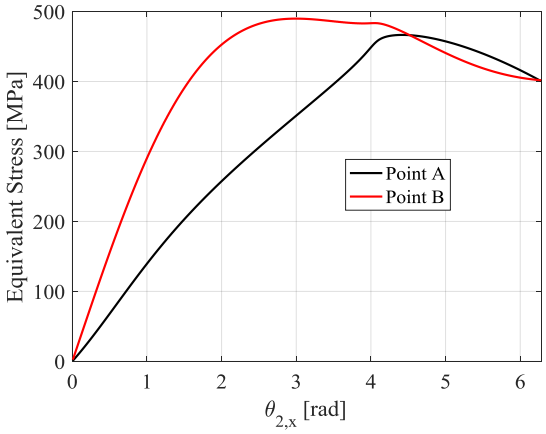


*Figure 6. Shows the equivalent stress in points of interest on the HFF during the folding process.*

Orientation of the principal stresses are analyzed during the folding process, and these are interesting when HFF is folded $\theta_{2,x} = \pi$. In this position the maximum and minimum principal stresses are orientated $\frac{\pi}{4}$ compared to the beam axis. This is easily seen on Fig. 7 where the vector principal stresses are illustrated, and the HFF is rotated $\theta_{2,x} \approx \pi$. That means that shear stresses are highly present in this part of the folding process. Orientation of the principal stresses is varying and both bending and shear appears during the folding process.

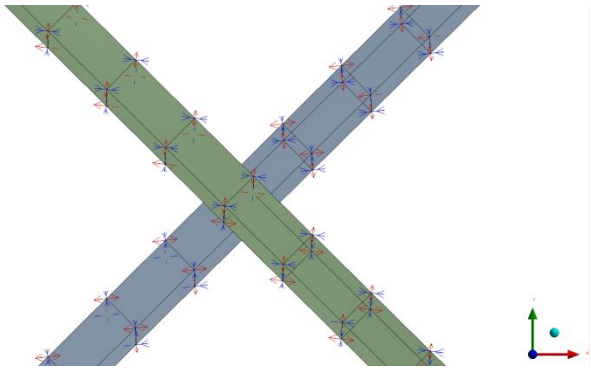

*Figure 7. The principal stresses are orientated as follows when the HFF is rotated $\theta_{2,x} \approx \pi$.*

In Fig. 8 the maximum principal stresses are illustrated and in point A, peaks the maximum principal stresses with 463 $MPa$ and in point B it peaks with 432 $MPa$. Compared to the equivalent stresses where point B was the critical point is it now point A when maximum principal stresses are compared. The maximum principal stress in point A is 16 % higher when it peaks compared to the maximum principal stress level when the HFF is folded.

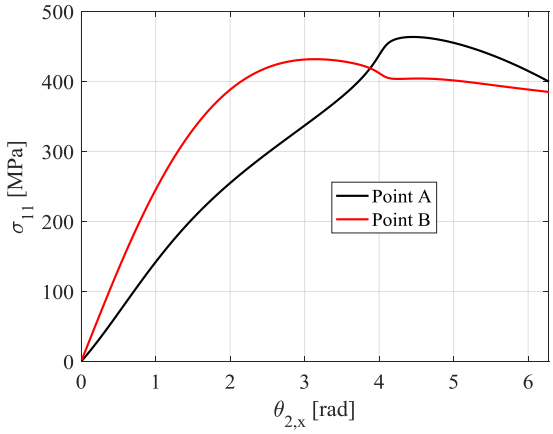


*Figure 8. Maximum principal stresses in the two points of interest during the folding.*

The non-linear behavior of the maximum principal stresses during the folding of the HFF is important to determine critical steps in the folding process.

## 5 DISCUSSION

The stresses determined from FEA are essential as these are required in an optimized design of the HFF. Stresses depend highly on the cross-sectional dimensions, and the diameter of HFF and the peak values are important to take into consideration. Other folding principles may reduce the stress peaks and therefore interesting to study. 9 foldings of the HFF is the next step in the process, and stress levels will increase significantly due to the folding of the HFF. Results from FEA depend highly on the boundary conditions applied the structure, and other boundary conditions can lead to higher or lower stress levels in the folding process.

## 6 CONCLUSIONS

From the results, it is proved that non-linear stress levels are present in the HFF during the folding process. These stress levels are important to know in the design of the HFF. Change in orientation of the principal stresses are identified, and these changes are important if an orthotropic material is used for the HFF. It is shown that a high $M_{R,x}$ not necesarely is equivalent to high principal stresses. It is proved that the equivalent stress levels during the folding process is higher than at the end of the folding process. When the HFF is folded, it is proved that the HFF is in a quasi-static state due to the nearly constant strain energy level.
From the analysis of pretension and stress stiffening is it now possible to make a dynamic analysis of the unfolding process. This process is an important part in further development of the SDSS.

## 7 ACKNOWLEDGEMENT

*SDSS is enhanced within the H2020 project TeSeR (Technology for Self-Removal). The goal of TeSeR is to take the first step towards the development of a scalable, flexible, cost-efficient, but highly reliable Post-Mission-Disposal (PMD) module. This module is to be attached to the spacecraft (S/C) on ground and it shall ensure the PMD of the S/C at the end of the nominal operational lifetime or act as a removal back-up in case that the S/C cannot be controlled anymore. This project has received funding from the European Union's Horizon 2020 research and innovation programme under grant agreement No 687295. [7]*

## 8 REFERENCES

1. Kristensen, A.S. & Damkilde, L. (2012). Self-deployable Deorbiting Space Structure. Patent, Pub.No.: WO/2012/092933.

2. Kristensen, A.S., Ulriksen, M.D. & Damkilde, L. (2017). *Journal of Spacecraft and Rockets, Vol. 54, No. 1. pp 323-326. Self-deployable Deorbiting Space Structure for Active Debris Removal.*

3. United Nations. (2010). Space Debris Mitigation Guidelines of the Committee on the Peaceful Uses of Outer Space. Online at *http://www.unoosa.org/pdf/publications/st_space_49E.pdf (As of January 2010 )*

4. Visagie, L., Lappas, V. & Erb, S. (2015). ScienceDirect. Acta Astronautica. *pp 65-75 Drag sails for space debris mitigation.*

5. Wiedemann, M. & Sinapius, M. (2013) *Adaptive, Tolerant and Efficient Composite Structures. (Eds. Martin. W. & Michael. Sinapius ). Springer.* pp. 237-249.

6. P. Frank Pai. (2007). *Highly Flexible Structures: Modeling, Computation and Experimentation. (Eds. Joseph A. Schetz). AIAA Education Series.* pp. 351-355.

7. Nikolajsen, J.A., Lauridsen P.R. & Kristensen A.S. (2017). 7th European Conference on Space Debris. ESA/ESOC, Darmstadt, Germany. *Modeling and analysis of the folding principle used in Self-deployable Deorbiting Space Structure.*